Phase-Coherent Frequency Combs in the Vacuum Ultraviolet via High-Harmonic Generation inside a Femtosecond Enhancement Cavity

R. Jason Jones,* Kevin D. Moll, Michael J. Thorpe, and Jun Ye†

JILA, National Institute of Standards and Technology and University of Colorado, Boulder, Colorado 80309-0440, USA

(Received 7 April 2005; published 20 May 2005)

We demonstrate the generation of phase-coherent frequency combs in the vacuum utraviolet spectral region. The output from a mode-locked laser is stabilized to a femtosecond enhancement cavity with a gas jet at the intracavity focus. The resulting high-peak power of the intracavity pulse enables efficient high-harmonic generation by utilizing the full repetition rate of the laser. Optical-heterodyne-based measurements reveal that the coherent frequency comb structure of the original laser is fully preserved in the high-harmonic generation process. These results open the door for precision frequency metrology at extreme ultraviolet wavelengths and permit the efficient generation of phase-coherent high-order harmonics using only a standard laser oscillator without active amplification of single pulses.

DOI: 10.1103/PhysRevLett.94.193201 PACS numbers: 39.30.+w, 42.62.Eh, 42.65.Ky

Recent developments in short-wavelength light sources have been rapid, with significant advances in temporal resolution, spectral coverage, and brightness [1,2]. A number of approaches have been proposed and/or are under active investigation, ranging from large scale systems such as free-electron laser-based x-ray generation [3] to smaller laboratory-based femtosecond amplifiers for high-harmonic generation (HHG) via photo-ionization dynamics, or extreme nonlinear optics [4,5]. However, the spectral resolution (or the corresponding temporal coherence) of these short-wavelength light sources remains poor in comparison with laser sources in the visible. Furthermore, system complexity and cost have prevented the widespread use of these short-wavelength light sources. In this work we address both issues using a standard femtosecond laser coupled to a completely passive optical cavity. Phase stabilization of a femtosecond optical frequency comb enables such a development.

Femtosecond laser-based optical frequency combs have played a remarkable role in precision measurement and ultrafast science [6]. Phase control of wide-bandwidth optical frequency combs has enabled numerous advances in optical frequency measurement and synthesis [7], optical atomic clocks [7,8], direct frequency comb spectroscopy [9], coherent pulse synthesis and manipulation [10], and deterministic studies in subcycle physics [1]. Phase stabilization of femtosecond pulses has also led to a certain degree of control capability in the HHG process, allowing generation of isolated, single attosecond pulses in the extreme ultraviolet (XUV) region [11]. However, the original frequency comb structure is lost due to the reduction of the pulse train repetition rate required to actively amplify single pulses to the energies needed for the HHG process. In this work we utilize phase stabilization of optical frequency combs as the necessary technological base for precise manipulation of femtosecond pulses such that they are coherently added inside a ''femtosecond (fs) enhancement cavity'' (Fig. 1). The enhanced intracavity field provides the necessary peak intensity for ionization of atoms or molecules for HHG where the liberated photoelectron recollides with the parent ion resulting in coherent light emission. The advances documented in this Letter enable a unification of these research fields, generating a high repetition rate (at the laser's original 100 MHz repetition frequency) and phase-controlled frequency comb in the XUV region, which is shown to maintain a definitive phase relationship with respect to the original comb in the near infrared. The spectral resolution demonstrated here can extend direct frequency comb spectroscopy [9] into the

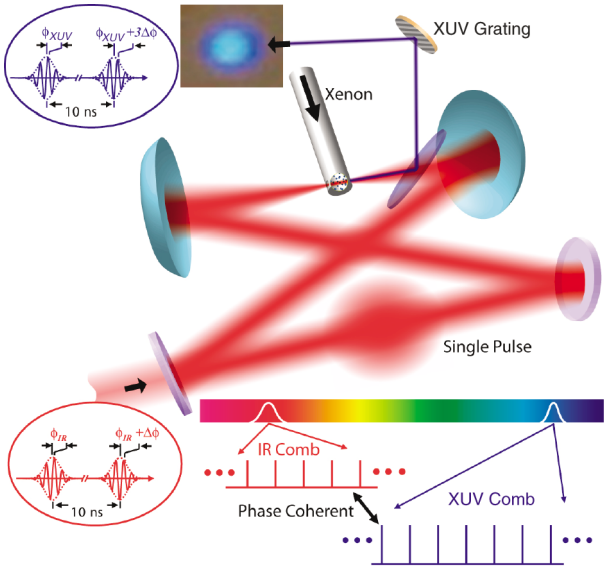

FIG. 1 (color). Schematic setup of intracavity high-harmonic generation. The incident pulse train is stabilized to a high finesse cavity, enhancing pulse energy nearly 3 orders of magnitude while maintaining a high repetition frequency. A gas target at the cavity focus enables phase-coherent HHG, resulting in a phase-stable frequency comb in the vacuum utraviolet (VUV) spectral region. The photo inset shows the actual spatial mode profile of the 3rd harmonic coupled out of the cavity.

XUV spectral region, advancing capabilities to perform high resolution spectroscopy [12], precision measurement [13], and coherent manipulation in the XUV. The inefficiency of the HHG process makes the fs enhancement cavity ideally suited for efficient harmonic generation as the driving pulse is continually ''recycled'' after each pass through the interaction region, leading to a significant improvement in the average power conversion efficiency compared to amplifier-based systems, up to the ratio in repetition rates (100's MHz compared to kHz). In addition, system cost and size are greatly simplified.

For successful implementation of this highly efficient approach to HHG, the passive optical cavity needs to demonstrate a number of important characteristics: (i) a high finesse to build up the pulse power, (ii) low round-trip group-delay dispersion to allow ultrashort pulses to be coupled into and stored inside the cavity, and (iii) a robust servo to stabilize the 2 degrees of freedom of the incident pulse train (e.g., optical carrier frequency and repetition frequency) to the corresponding cavity resonance modes. We have been pushing towards these goals for the past several years, investigating direct stabilization of femtosecond lasers to high finesse cavities [14], dispersion compensation and characterization of mirror coating technology [15], and the nonlinear response of the cavity to intracavity elements [16]. The previous work resulted in the demonstration of passive-cavity-based ''amplifiers'' in both picosecond [17] and femtosecond [18] regimes by periodically switching out the stored intracavity pulse.

A standard mode-locked femtosecond Ti:Sapphire laser with a repetition frequency (f_r) of 100 MHz, 48 fs pulse duration, and 8 nJ pulse energy is used. The carrier-envelope offset frequency (f_0) and f_r set the pulse-to-pulse carrier-envelope phase evolution as $\Delta\phi = 2\pi f_0/f_r$ (Fig. 1). The pulse train from the laser passes through a prism-based compressor before incident on the passive optical cavity. To couple the pulse train from the mode-locked laser into the cavity, both f_0 and f_r of the laser are adjusted such that the optical comb components are maximally aligned to a set of resonant cavity modes [15]. For short optical pulses (<100 fs) and high finesse cavities ($F > 1,000$), the comb components need to overlap with corresponding narrow cavity resonances across a large spectral bandwidth. The power transmitted through the cavity as the length of the laser is scanned therefore shows a single sharp resonance only when both the laser carrier frequency (average comb position) and spacing (f_r) are optimally aligned [Fig. 2(a)] [19].

To investigate the peak intensity that can be obtained with this method, an empty fs enhancement cavity was initially characterized. The passive optical cavity has a ring geometry formed by six mirrors. All mirrors are high reflectors except the input coupler, which has a transmission of 0.1%, nearly matching the net intracavity loss. The center wavelength of the mirror coating is 800 nm, with a bandwidth of 100 nm within which the net cavity group-delay dispersion is compensated to <10 fs^2. However,

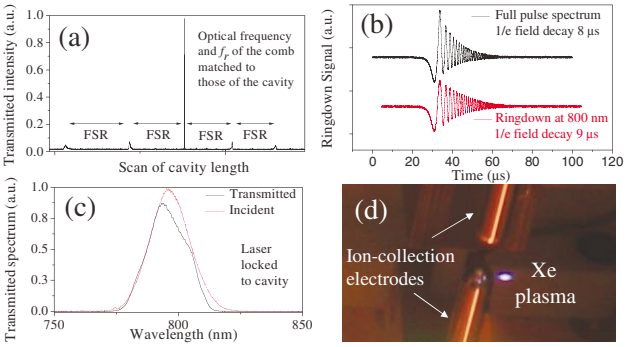

FIG. 2 (color). Characterization and measurement of the fs enhancement cavity. (a) Transmission through fs enhancement cavity as the laser cavity length is scanned. The dominant peak results from optimal alignment of frequency comb modes to resonant modes of the fs enhancement cavity. (b) Cavity ring-down measurements for the entire pulse spectrum (top trace) and for a 5 nm region centered at 800 nm. (c) Incident and transmitted spectrum of the pulse. The pulse durations measured by frequency-resolved-optical gating are 48 fs (incident) and 60 fs (transmitted). (d) Visible plasma generation at the cavity focus. A pair of electrodes for ion collection is useful for signal optimization.

residual group-delay dispersion in the enhancement cavity causes the cavity free-spectral-range (FSR) frequency to vary as a function of wavelength, limiting the bandwidth of the pulse that can be coupled into the cavity [15]. To measure the average cavity finesse, a ring-down measurement of the cavity field decay is performed across the bandwidth of the laser pulse. The ring-down signal is measured in reflection from the cavity, in the form of an optical heterodyne beat between the leakage field from the cavity and the incident field reflected off of the input coupler [7]. The decay curve gives a cavity field decay time of ≈ 8 μs for the entire pulse bandwidth [Fig. 2(b)], corresponding to an effective finesse of 2500. The ring-down time of a few comb components centered at 800 nm is ≈ 9 μs, consistent with the predicted cavity finesse of 3000 at the center wavelength of the coating.

The average frequency of the laser is locked to the fs enhancement cavity by adjusting the cavity length. A second servo loop, actuated on the group delay inside the laser cavity, keeps the transmission peak maximized by controlling f_r [14,20]. As we will show later, this phase stabilization of the near-IR femtosecond comb directly transfers the resultant phase stability to that of the HHG light. The transmitted spectrum indicates the deleterious effect of the cavity dispersion limiting the intracavity pulse bandwidth [Fig. 2(c)]. By measuring the transmitted pulse while adjusting the compressor, it is verified that the minimum compressable pulse duration inside the cavity is 60 fs. The intracavity pulse energy is enhanced up to 4.8 μJ for these short pulses, approximately a 600-fold increase from the incident pulse energy of 8 nJ. Based on these measurements we estimate a peak intracavity intensity of $>3 \times 10^{13}$ W/cm^2 is produced at the intracavity focus.

We have verified experimentally that the ionization required in the HHG process does not degrade the effective cavity finesse at the intensities and pressures used here. Noble gas atoms, such as Xe or Kr, as well as N_2 molecules, are introduced at the cavity focus (Fig. 1). A ≈ 25 μm beam waist is formed between the curved mirrors (radius of curvature 10 m), where peak intracavity intensities exceed ionization thresholds of Xe and Kr, producing a strong visible plasma [Fig. 2(d)]. For optimization of the intracavity intensity, a pulse compressor is adjusted to minimize the intracavity pulse duration by monitoring the relative ionization strength via a pair of electrodes.

To couple the copropagating HHG light out of the cavity without affecting the finesse for the 800 nm comb, a ~ 700 μm-thick fused-silica or sapphire plate is placed at Brewster's angle for the IR inside the cavity (Fig. 1). This additional optical element, while lowering the cavity finesse by $<5\%$, requires a negative group-delay-dispersion coated mirror to compensate for the additional material dispersion. Higher order dispersion in the cavity still increases slightly and the useful bandwidth of the cavity is thus reduced by a small amount. However, it does not produce a noticeable difference in the transmission spectrum shown in Fig. 2(c). The Fresnel reflection coefficient of the intracavity plate rises towards shorter wavelengths in the XUV, with a maximum reflectivity of $\sim 10\%$ between 30 to 80 nm. For the coherent detection of the comb structure of the HHG light at 266 nm (3rd harmonic) discussed later, this intracavity plate is coated to provide a reflectivity of $\sim 40\%$ at that wavelength.

The gas target is confined within a thin, hollow brass cylinder, with a 150 μm hole to allow the intracavity pulse to pass through (Fig. 1). The 0.75 mm inner diameter of the tube defines the effective interaction length of the gas target. The typical backing pressure is about 30 Torr, with <1 mTorr of background pressure for the evacuated chamber where the fs enhancement cavity is located. The position of the gas target is adjusted to be slightly after the cavity focus to maximize the HHG light. While Kr atoms and N_2 molecules have both produced HHG light, Xe is used for the data presented throughout this Letter. The diffracted pattern of the HHG light, obtained with a MgF_2-coated aluminum grating, demonstrates that at least the 7th order harmonic is generated (Fig. 3). While the low detection efficiency of this system limits the harmonics observed so far, we expect the spectrum should extend well into the XUV spectral region considering recent results on anomalous high-order harmonic generation obtained at similar intensity levels [21]. Similar work in Garching has recently demonstrated HHG up to the 15th harmonic [22]. The average power of the 3rd harmonic light generated inside the cavity reaches nearly 10 μW. The corresponding intracavity single-shot efficiency ($\approx 10^{-8}$) is comparable to traditional femtosecond-amplifier-based systems at similar intensity levels. This demonstrates the dramatic increase in high-harmonic power that can be accessed using a high repetition rate (100 MHz). Clearly

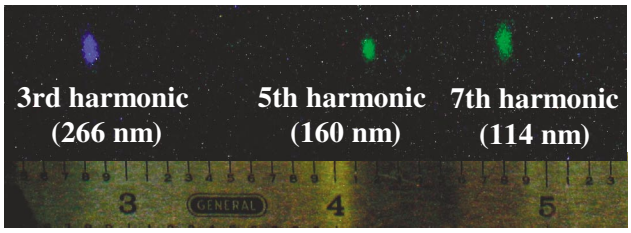

FIG. 3 (color). Detection of the 3rd, 5th, and 7th harmonic signals on a phosphor screen after diffraction from a grating.

there is significant potential to further improve this efficiency and produce harmonics far into the XUV simply by increasing the incident pulse energy, easily allowing access to intensities $>10^{14}$ W/cm^2 at high repetition rates. A number of attractive oscillators include an extended cavity femtosecond Ti:sapphire laser [23] or Yb-doped yttrium aluminum garnet (Yb:YAG) mode-locked laser that produce pulse energy above 1 μJ directly from the oscillator [24]. A potential limitation for scaling up the intracavity intensity with this approach is the presence of an observed nonlinear response of the intracavity plate, which has been reported in previous experimental and numerical work [14,16]. A possible configuration to overcome this limitation is to use a higher order spatial mode of the cavity and couple the generated XUV light out via a small hole (≈ 100 μm diameter) drilled in the second curved mirror. This separation of HHG light from the fundamental beam via diffraction has already been demonstrated in amplified systems with annular laser beams [25]. This cavity configuration can allow efficient output of all HHG orders and permit scaling up the technique to greater intracavity intensities.

The fs enhancement cavity provides an ideal platform to perform detailed studies of phase coherence of the HHG process. First, the high repetition frequency makes it possible to have a well-separated frequency comb structure that would allow a direct optical heterodyne detection of the comb linewidth. Second, the fs cavity provides ideal spatial filtering for the input fundamental pulses, as well as phase and amplitude stabilization of the input pulses. One strategy to determine the coherence properties of the HHG process is to have a suitable narrow-linewidth continuous-wave laser in the XUV region to heterodyne beat against the XUV comb and produce a coherent beat signal, as is normally done for the visible optical frequency comb work. Another strategy is to use two sets of XUV combs and bring them together for coherent interferometry by detecting the heterodyne beat between them. To directly measure any phase or frequency fluctuations in the harmonic generation process, we allow the original comb to drive two independent nonlinear processes, one through the usual perturbative nonlinear optics based on second harmonic and sum frequency generations via two beta-barium-borate (BBO) optical crystals and the other through the intracavity HHG process. Two sets of the frequency

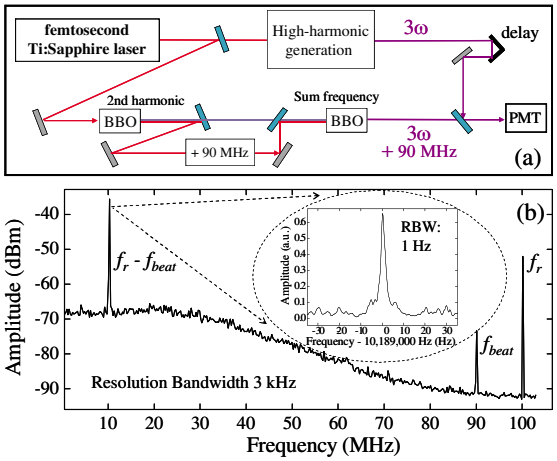

FIG. 4 (color online). (a) Setup for coherent heterodyne detection between 3rd harmonic generated in Xe gas and that generated by bound optical nonlinearities in BBO. (b) Measurement of the detected beat signal and repetition frequency. The linewidth shown in the inset is resolution bandwidth limited at 1 Hz.

combs at 266 nm that represent the third harmonic of the fundamental IR comb are then brought together in a Mach-Zehnder interferometer geometry [Fig. 4(a)] for beat detection, after these two separate pulse trains are temporally overlapped. A 90 MHz acousto-optic modulator is inserted in one of the interferometer arms so that the beat detection is shifted to a convenient nonzero frequency. Pairs of corresponding comb components from each spectrum produce coherent optical beats, which collectively add together to form the beat signal detected by a photomultiplier. The radio frequency spectrum of the beat note shows the clear presence of the comb structure in the UV [Fig. 4(b)], with a repetition frequency signal at 100 MHz and coherent beat signals both at 90 MHz and 10 MHz. The high frequency roll-off is due to the response function of the photomultiplier amplifier. The resolution bandwidth-limited 1 Hz beat signal [inset, Fig. 4(b)], influenced by slow, differential path length fluctuations of the interferometer, demonstrates that the full spectral resolution and temporal coherence of the original near-IR comb has been faithfully transferred to higher harmonics in the HHG process, limited only by the observation time period of $\sim$1 s.

This type of temporal coherent interferometry of the HHG light opens the door for an exciting and unique set of precision measurements on the HHG process. While the present test relying partially on bound optical nonlinearities is limited to the 3rd harmonic, two independent fs enhancement cavities can be easily implemented and will allow the same type of coherent optical heterodyne measurements to be performed at any harmonic order in the XUV spectral range. This ultrahigh spectral resolution approach will allow precise, phase-sensitive measurements of long and short quantum trajectories [26,27] associated with freed electrons during the HHG process, as proposed in the 3-step model [4,5]. A number of physical processes that impact the phase coherence properties of HHG can be studied in detail, including ionization dephasing, intensity-dependent phase shifts, the effect of temporal chirp (spectral phase) of the near-IR pulse on the HHG light, etc., In the future, the presence of the frequency comb structure in the VUV and XUV spectral regions will enable similar advances in precision measurement, quantum control, and ultrafast science as have been recently witnessed in the visible region.

We thank D. Dessau and J. L. Hall for equipment loans, R. Lalezari (Advanced Thin Films) for mirror coatings, and J. Biegert for useful discussions. The work is supported by AFOSR, ONR, NASA, NIST, and NSF.

*Electronic address: rjjones@jilau1.colorado.edu
†Electronic address: Ye@jila.colorado.edu

[1] R. Kienberger and F. Krausz, in *Few-Cycle Laser Pulse Generation and Its Applications*, Topics in Applied Physics, Vol. 95 (Spring, New York, 2004), p. 343.
[2] A. Endo, IEEE J. Sel. Top. Quantum Electron. **10**, 1298 (2004); E. J. Takahashi *et al.*, IEEE J. Sel. Top. Quantum Electron. **10**, 1315 (2004); E. A. Gibson *et al.*, IEEE J. Sel. Top. Quantum Electron. **10**, 1339 (2004); K. A. Rosfjord *et al.*, IEEE J. Sel. Top. Quantum Electron. **10**, 1405 (2004).
[3] H. Wabnitz *et al.*, Nature (London) **420**, 482 (2002).
[4] P. B. Corkum, Phys. Rev. Lett. **71**, 1994 (1993).
[5] M. Lewenstein *et al.*, Phys. Rev. A **49**, 2117 (1994).
[6] T. Udem *et al.*, Nature (London) **416**, 233 (2002); S. T. Cundiff *et al.*, Rev. Mod. Phys. **75**, 325 (2003).
[7] J. Ye, H. Schnatz, and L. W. Hollberg, IEEE J. Sel. Top. Quantum Electron. **9**, 1041 (2003).
[8] S. A. Diddams *et al.*, Science **293**, 825 (2001).
[9] A. Marian *et al.*, Science **306**, 2063 (2004).
[10] R. K. Shelton *et al.*, Science **293**, 1286 (2001).
[11] A. Baltuska *et al.*, Nature (London) **421**, 611 (2003).
[12] M. Bellini, S. Cavalieri, C. Corsi, and M. Materazzi, Opt. Lett. **26**, 1010 (2001); S. Witte *et al.*, Science **307**, 400 (2005).
[13] S. D. Bergeson *et al.*, Phys. Rev. Lett. **80**, 3475 (1998).
[14] R. J. Jones, I. Thomann, and J. Ye, Phys. Rev. A **69**, 051803 (2004).
[15] M. J. Thorpe *et al.*, Opt. Express **13**, 882 (2005).
[16] K. D. Moll, R. J. Jones, and J. Ye, Opt. Express **13**, 1672 (2005).
[17] E. O. Potma *et al.*, Opt. Lett. **28**, 1835 (2003).
[18] R. J. Jones and J. Ye, Opt. Lett. **29**, 2812 (2004).
[19] R. J. Jones, J. C. Diels, J. Jasapara, and W. Rudolph, Opt. Commun. **175**, 409 (2000).
[20] R. J. Jones and J. C. Diels, Phys. Rev. Lett. **86**, 3288 (2001).
[21] C. Valentin *et al.*, Appl. Phys. B **78**, 845 (2004).
[22] C. Gohle *et al.*, Nature (to be published).
[23] A. Fernandez *et al.*, Opt. Lett. **29**, 1366 (2004).
[24] T. Sudmeyer *et al.*, Opt. Lett. **28**, 1951 (2003).
[25] J. Peatross, J. L. Chaloupka, and D. D. Meyerhofer, Opt. Lett. **19**, 942 (1994).
[26] R. Zerne *et al.*, Phys. Rev. Lett. **79**, 1006 (1997).
[27] M. Bellini *et al.*, Phys. Rev. Lett. **81**, 297 (1998).